

PID-MMAC using an approximate H_∞ loop-shaping metric

Rakesh Joshi * Victoria Serrano ** Konstantinos Tsakalis*

* *School of Electrical, Computer and Energy Engineering, Arizona State University, Tempe, AZ 85281, USA*

** *Electrical Engineering Department, Universidad Tecnologica de Panama, Lasonde, West 6th Avenue, David, Chiriqui, Panama*

Abstract: This paper proposes a PID-multi-model adaptive control (PID-MMAC) algorithm using an approximate H_∞ metric that represents the frequency loop-shaping (FLS) cost objective. Existing MMAC algorithms use L_2 or least squares-based cost functionals on a suitable error signal to perform controller switching, but their strong dependency on the properties of the excitation makes them sensitive to noise, disturbances and modeling errors. Alternatively, a system-norm-based cost function is advantageous for MMAC as it is less sensitive to the specific signals used for adaptation. In this paper, the H_∞ norm in the FLS cost objective is approximated by frequency decomposition of the real-time signals using filter-banks. An MMAC algorithm using this metric is presented and its application to controller switching is discussed. The buck converter serves as the motivating application where the adaptation seeks to compensate for degradation in its components (inductors and capacitors). A comparative study is conducted of the proposed algorithm and an L_2 -based MMAC algorithm under various excitation conditions. The results show that the proposed algorithm is less susceptible to the properties of the excitation signals as compared to the least squares-based MMAC.

Keywords: MMAC-Multi model adaptive control, FLS- frequency loop shaping, RSC-robust stability condition

1. INTRODUCTION

Proportional-Integral-Derivative (PID) controllers are a widely used class of controllers in industrial processes, electric circuits and in mechanical systems. Low dimensionality of the controller, variety of readily available tuning methods and ease of implementation by electronic circuits using op-amps make them popular as compared to other classes of controllers. Åström and Hägglund (1995), Åström and Hägglund (2006), Rivera et al. (1986) provide review of various methods used in design and implementation of PIDs. Even though a well tuned fixed PID controller yields good performance around an operating point, it may fail to compensate for the nonlinearities and time-varying characteristics perturbing the nominal plant. To overcome this shortcoming, the adaptation of PID parameters is a favorite candidate solution.

Adaptive control is an extensively researched field with many adaptive control schemes studied in the literature. Some of them are gain scheduling, multi-model adaptive control e.g., Stefanovic and Safonov (2008), Anderson et al. (2001), Hespanha et al. (2001), Hespanha and Morse (1996), Anderson et al. (2000), model reference adaptive control and indirect adaptive control, e.g., Sastry and Bodson (2011), Ioannou and Sun (1996). Interest in multi-model adaptive control (MMAC) has gained traction significantly in recent past. In this scheme, the controller used in the closed-loop system is selected from a bank of controllers based on metrics derived from the on-line data.

In a brief review, the theoretical framework of the data-driven MMAC algorithms seeking robust stability and safe switching is discussed in Stefanovic and Safonov (2008), Buchstaller and French (2016a), Buchstaller and French (2016b), Sajjanshetty and Safonov (2014). A multi-variable MMAC algorithm using an estimator and a controller that can tolerate structural uncertainties is discussed in Tan et al. (2016). The application of MMAC in pH control is discussed in Böling et al. (2007) and refinement of this algorithm for a noisy environment is discussed in Bashivan and Fatehi (2012). All these MMAC methods use error signals that represent prediction or control error or their combination, to compute the metric used in the controller switching and their cost functionals are signal-norms of the error signals.

In this paper, we discuss the development of an alternative to the usual update laws that is based on the approximation of system norms as cost functionals, instead of signal norms. The general adaptation of MMAC schemes uses a metric derived from the on-line data for the selection of the controller from a bank of controllers C_i and can be written as follows

$$C^* = \arg \min_{C_i} J(C_i; x) \quad (1)$$

Where C_i denotes controller from the controller bank, x denotes measured signals and $J(C_i, x)$ is the cost functional associated with a metric used in the controller switching. Typical cost functionals are the mean square error or exponentially weighted mean square error, where the error represents difference between expected and actual

response (ex. prediction error, control error etc.). If the signals are persistently exciting, there is no noise or disturbances, and the controller bank is appropriately selected, such an adaptive law produces optimal performance. However, perturbations such as sensor noise and disturbances result in a cost functional whose minimum can be significantly different depending on the signals at hand (e.g., see Tsakalis (1996)) and whose consequence is often poor performance or adaptation bursts. Furthermore, the worst-case performance depends on the parametric uncertainty and the problem is not easily detected with a “noisy simulation”. This may provide a false sense of security, which is further exacerbated in the MMAC case where one considers only a small number of controllers. Potential partial remedies for this problem have been recognized in the incorporation of dead-zones in the adaptive law but their design is far from providing a complete practical answer.

In an effort to design an adaptation cost functional that provides a better description of our control objective, hence resulting in a weaker dependence on signal properties, we propose the approximation of the norm of an error system. An example of such an error system is the difference between the actual loop and its target, arising in frequency loop-shaping. Controllers based on the optimization of such objectives have quantifiable robustness properties that have constituted the cornerstone of the development of robust control theory since the 80’s. While robust control objectives have often been used in adaptive controllers, our approach is different in that we incorporate them in the estimator (or optimizer) and not just in the derivation of the control law.

A general description of one such cost functional can be broadly described as follows:

$$C^* = \arg \min_{C_i} \max_x J(C_i; x) \quad (2)$$

The above structure allows us to describe cost functional in terms of the worst-case behavior of each controller and the selection of the controller is the one that produces minimum worst-case behavior. Motivated by the results of the H_∞ robust control theory, we consider the decomposition of the cost function in terms of the frequency components of the signal x :

$$C^* = \arg \min_{C_i} \max_j J(C_i; x_j) \quad (3)$$

where now x_j represents the energy of measured signals at different frequency directions and $J(\cdot)$ is a system norm. The former can be achieved under a linearity assumption by processing the input and output signals through “filter banks” (FB), an example of which is shown in Fig. 1. In this manner, the signal decomposition may only approximate its frequency content, but it is exact at all times and does not suffer the usual windowing effects of Fast Fourier transforms (FFT). On the other hand, a system norm computation would require the normalization of the system output RMS power by the corresponding input power, something that is achievable by requiring excitation that is persistent and of sufficient magnitude.

Thus, the proposed approach enables the approximation of an H_∞ cost functional using a single data sequence. Its main drawbacks are in the dimensionality of the solution and the excitation requirements. We must point

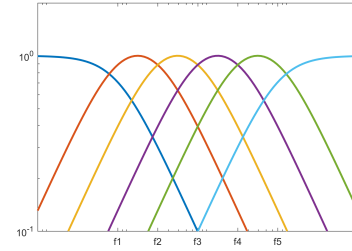


Fig. 1. Bode diagram of a filter bank

out, however, that neither one represents insurmountable limitations for many practical cases. With the advances in computing hardware and parallel implementations, the use of filter-banks of band-pass filters is a viable alternative to FFT algorithms. And excitation is often present in practical problems, or can be requested for short time periods, and can at least be verified by a monitoring program before updating the controller parameters. The same monitoring logic can also limit the use of excitation directions to the ones that contain sufficient excitation, e.g., through the use of an adaptation dead-zone. It is our view that the critical part of adaptive control is the ability of the adaptation to take advantage of short or occasional excitation periods in the most efficient way, instead of attempting to operate with the least assumptions but opening the door to undesirable nonlinear behavior like bursting.

Over the past two decades, we have employed the FLS approach for PID controller tuning with excellent results in a variety of practical problems. In FLS the specifications for the closed-loop system are expressed in terms of the target loop and the PID parameters are obtained by solving a minimization of a distance metric between the actual loop and the target loop, defined in terms of an H_∞ norm. The off-line FLS algorithm for PID tuning is discussed Tsakalis et al. (2002) Grassi and Tsakalis (2000). An on-line version of FLS algorithm for tuning PID parameters with an approximate H_∞ cost functional is discussed in Tsakalis and Dash (2013), while an extension and application to performance monitoring is presented in Tsakalis and Dash (2007). We use this FLS-based approximate H_∞ metric in the development of our proposed MMAC algorithm.

In the rest of this paper we present some details on the formulation of this problem and its computation for a PID control structure (Section 2). We also discuss some of the typical characteristics of the solution, applied to the PID control of a buck converter. Buck converters with a fixed, op-amp-based PID controller are commonly used in the regulation of DC voltage. However, the degradation of its components (e.g., inductor or capacitor) causes regulation performance to deteriorate beyond the capabilities of the fixed PID controller. This specific application is of particular interest for MMAC since common implementations can include banks of resistances that can be used to switch among a finite number of controllers (Section 3). Using this as a case study, we demonstrate the application of the proposed MMAC and compare with the results obtained with existing approaches. The novelty of the contribution is in the usage of the approximate H_∞ metric in the formulation

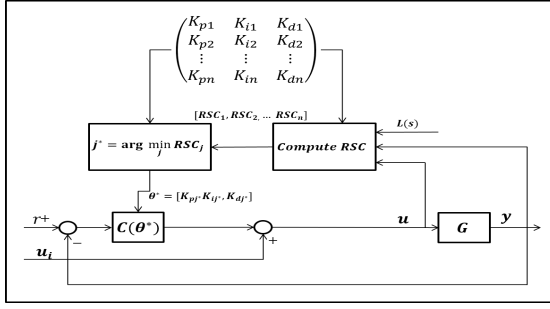


Fig. 2. MMAC schematic diagram

of the MMAC algorithm and a systematic construction of a test example that shows its low susceptibility to parameter misadjustment and burst phenomena caused by variations in the signal excitation.

2. MULTI-MODEL ADAPTIVE CONTROLLER

Letting G be the plant and C the controller, the FLS objective is to minimize the distance between the loop transfer function GC and the target loop L . A frequency-weighted version of this distance is obtained by the application of the Small Gain Theorem, yielding the robust stability condition (RSC)

$$\|S(GC - L)\|_\infty < 1 \quad (4)$$

Where $S = 1/(1+L)$ is the target sensitivity. The left-hand side of Eq. 4 can be interpreted as a particular, closed-loop-relevant, distance between the target and actual loops and $\|S(GC - L)\|_\infty$ is the FLS optimization objective. A desirable feature of this RSC metric is that it is normalized such that a value less than 1 guarantees closed-loop stability. Furthermore, while it is not explicitly a robust performance metric, small values of the RSC (e.g., 0.1-0.3) indicate a practically close matching between the nominal and the actual loop sensitivities.

Next, consider a parameterization of the PID controller as

$$C(s; \theta) = K_p + \frac{K_i}{s} + \frac{K_d s}{\tau s + 1} \quad (5)$$

where $\theta = [K_p, K_i, K_d]$ are the PID parameters proportional, integral, and derivative gains, respectively, and τ is the time constant of the filter used in the implementation of derivative control and its value is chosen a priori. For this PID parameterization the RSC minimization problem is convex, and, in fact, linear in the parameters θ :

$$\theta^* = \arg \min_{\theta \in M} \|S(GC(\theta) - L)\|_\infty \quad (6)$$

Here $\theta \in M$ are convex parameter constraints, e.g., positivity of the PID gains, or a minimum phase condition to avoid right half-plane cancellations. The quality of the approximation of the target by the PID loop can be assessed by looking at the optimal RSC value. If it is less than 1, the stability of the closed-loop system is guaranteed and lower values of optimal RSC implies the actual loop-performance closer to the target. The convergence of the FLS method to reasonable PID tunings, as compared to standard methods in the literature, e.g., Åström and Hägglund (1995) Åström and Hägglund (2006) Rivera et al. (1986), has been established in Grassi and Tsakalis (2000).

To convert this method for on-line use, we let (u, y) be the input-output pair of the plant and define the error signal

$e = S(CG - L)u$; invoking the fact that $y = Gu$, we obtain $e = SCy - Tu$. Thus, the RSC can be expressed as:

$$RSC = \|S(CG - L)\|_\infty = \sup_{\|u\| \neq 0} \frac{\|e\|_2}{\|u\|_2} \quad (7)$$

Using filter banks of band-pass filters F_i to decompose the signals, and we arrive the following estimate of RSC

$$RSC \approx \max_i \frac{\|F_i e\|_{2,\delta}}{\|F_i u\|_{2,\delta}} = \max_i \frac{\|SCF_i y - TF_i u\|_{2,\delta}}{\|F_i u\|_{2,\delta}} \quad (8)$$

Here we also use the exponential weighted exponential norm $\|x\|_{2,\delta} = \{\int_{-\infty}^{\infty} e^{2\delta t} |x|^2(t) dt\}^{\frac{1}{2}}$, $\delta > 0$ in the computation of upper bound of RSC approximation. This allows for the recursive and efficient computation of RSC as the ratio of the outputs of two first order filters.

This approximation is similar to an FFT decomposition of the signal when the filter bank is composed of sharp bandpass filters. In a strict sense it is only a lower bound of the actual RSC because it is computed for a finite number of signals. However, for reasonably smooth practical problems, a good approximation can be achieved with a modest number of band-pass filters. The significance of this formulation is the PID tuning can be achieved in the sense of system norms, having reduced sensitivity to the actual frequency content of the signals. Furthermore, the use of normalized quantities that are motivated by the Small-Gain Theorem means that the confidence in the adaptation can be assessed (by a supervisory system) in terms that are problem independent.

2.1 RSC based PID-MMAC algorithm

In a quick overview, MMAC uses the plant input-output data to estimate a performance or health metric, assessing the suitability of a controller in the loop. This metric is then used to rank the potential controllers and switching to the best candidate. The key difference of the proposed metric is in the approximation of the H_∞ gain of the mismatch operator, instead of the more frequently used L_2 -norm of the error signal. Our expectation, supported by simulation studies, is that the proposed metric would translate in a reduced sensitivity of the optimal solution to the input signal properties and in a more reliable performance.

For the MMAC problem, we consider the bank of plants $[G_j], j = 1, 2, \dots, n$, and a corresponding bank of controllers $[C_j]$, designed with an off-line FLS algorithm and with a target loop-shape L . The RSC estimate of each controller C_j is computed using the plant input-output data according to Eq. 8 and is denoted by RSC_j . (Here, it helps to evaluate the controllers using the same criterion as for their design.) The objective of a multi-model adaptive switching control is to select the controller that minimizes the estimated RSC, which can thus be written as the following optimization problem:

$$C_j^* = \arg \min_{C_j} \max_i \frac{\|SC_j F_i y - TF_i u\|_{2,\delta}}{\|F_i u\|_{2,\delta}} \quad (9)$$

Although the above switching logic can be used with any type controllers, the PID structure (Eq. 5) enables us to draw on the extensive available insight to design the filter banks and determine the set of reasonable controllers. For the PID-MMAC, the parameter adaptation becomes

$$\theta_{j^*} = \arg \min_{\theta_j} \max_i \frac{\|(SF_i W^T y)\theta_j - TF_i u\|_{2,\delta}}{\|F_i u\|_{2,\delta}} \quad (10)$$

where $W = [1; \frac{1}{s}; \frac{s}{\tau s + 1}]$ and $\theta_j = [K_{pj} K_{ij} K_{dj}]^T$ are the parameters of the controller C_j (Eq. 5). To avoid excessive switching, a common approach is to introduce a switching threshold or a hysteresis logic, trading off transient performance for a less oscillatory behavior.

Thus, the PID-MMAC algorithm, based on the approximation of the H_∞ RSC, becomes:

- Design PID controllers $[C_j]$ for the set of plants G_j for the selected the target loop $L(s)$.
- Initialize to the nominal controller.
- For each time step k , compute the RSC values for all controllers $[C_j]$

$$RSC_j(k) = \max_i \frac{\|SF_i W^T y\theta_j - TF_i u\|_{2,\delta}}{\|F_i u\|_{2,\delta}} \quad (11)$$

- If $RSC_{selected} > (1 + h) \min_j RSC_j(k)$, then switch to the controller $C(\theta_{j^*})$, where $RSC_{selected}$ is the RSC value of the currently selected controller, $j^* = \arg \min_j RSC_j(k)$ and h is a hysteresis parameter ($h > 0$).

The evaluation of the RSC metric (as all similar metrics) involves the inherent trade-off between the long and short term memory. The former has noise immunity while the latter offers fast adaptation to rapidly changing conditions. In our case, a comparison between the estimated exponentially weighted norm and the actual 2-norm of the RSC indicates that a value $\delta = BW/10$, where BW is the bandwidth of target loop transfer function is a reasonable choice.

The RSC computation also needs to handle the possibility of insufficient excitation. The disturbance threshold term described in Tsakalis and Dash (2007) can be used in the RSC computation to avoid bias in the RSC values because of lack of excitation. To avoid bias in the parameter estimate because of disturbances or noise, the plant input-output pair used in the RSC estimation is filtered using a band pass filter that only allows signals in the frequencies of interest, namely around the loop crossover frequency.

3. PID-MMAC DESIGN FOR A BUCK CONVERTER

A schematic diagram of a buck converter is shown in Fig. 3. It consists of a MOSFET, a LC circuit with a power inductor (H) and capacitor (Q) and the goal of the converter is to regulate the voltage across the resistive load to a set-point by controlling gate of MOSFET. The MOSFET gate is controlled by varying the duty cycle of a pulse-width-modulated (PWM) signal and an op-amp-based PID controller is typically employed to generate the PWM signal based on the output voltage measurement. Degradation in the inductor and capacitor components can result in the degradation of the performance of the buck converter, which the fixed PID may be unable to compensate.

To solve this problem, multiple PID controllers can be made available, e.g., through a resistor bank, with a MMAC algorithm used in the selection the best controller.

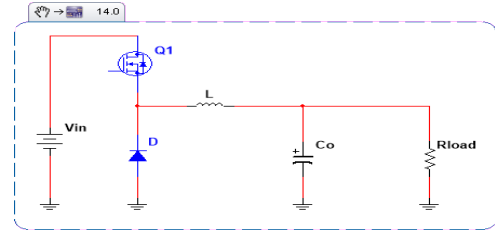


Fig. 3. Schematic diagram of a buck converter

In this section, we show the results from application of the proposed MMAC in the buck converter and we also demonstrate pros and cons of MMAC using the proposed approximate H_∞ cost functional over the standard, signal-based, L_2 cost functionals. Details of the buck converter components and justification for their selection are discussed in Serrano (2016). For this study we restrict ourselves to transfer functions of the buck converter derived using first principles with degradation in its components. It can be also seen from Serrano (2016) that degradation in the capacitor and inductance only affects the resonance frequency ($f_o = \frac{1}{\sqrt{HQ}}$) of the buck converter's transfer function, so for this study we only consider combined degradation in capacitance and inductance.

The transfer functions of the buck converter with the percent degradation in its components from the nominal are listed below. The frequency units are $rad/\mu sec$

- 0 percent: $G_1 = \frac{0.0098(s+14.29)}{(s^2+0.1419s+0.2778)}$
- 20 percent: $G_2 = \frac{0.01535(s+14.29)}{(s^2+0.1774s+0.4341)}$
- 40 percent: $G_3 = \frac{0.0273(s+14.29)}{(s^2+0.2365s+0.7717)}$
- 50 percent: $G_4 = \frac{0.04(s+14.29)}{(s^2+0.2838s+1.111)}$
- 60 percent: $G_5 = \frac{0.0614(s+14.29)}{(s^2+0.3548s+1.736)}$

The target loop shape is selected to achieve a closed-loop bandwidth $0.7 rad/\mu sec$ and is used to tune PID controllers. Its transfer function is:

$$L(s) = \frac{0.65019(s^2 + 0.467s + 0.2531)}{s(s^2 + 0.1419s + 0.2778)} \quad (12)$$

which includes resonance characteristics from the plant, since a PID by itself has no degrees of freedom to alter plant zeros. (Also see Grassi and Tsakalis (2000), Tsakalis et al. (2002) for comments on target selection.) Finally, the MMAC controller bank is formed using PID controllers designed for the above-listed plants, with a derivative time constant $\tau = 0.01$ and for the target loop-shape $L(s)$ (Eq. 12). We also include some spurious controllers in the controller bank and PID parameters of all controllers in Table 1 to demonstrate the difference of parameter misadjustment in system-norm and signal-norm adaptation.

4. MMAC RESULTS

To test the proposed MMAC algorithm, the plant with no degradation G_1 is switched to a plant with degradation (G_2 - G_5) at 400 micro seconds. Excitation for the adaptation algorithms is defined as a square wave ($-5V$ to $+5V$) in the reference signal and a sine wave (magnitude $0.2V$) with different frequencies is injected at the plant input (u_i in Fig 2) as a disturbance. White noise is also added at

Table 1. PID gains for the buck converter controller bank.

Controller	K_p	K_i	K_d	Comments
C_1	2.007	1.185	4.559	Controller designed for plant G_1
C_2	1.062	1.232	2.835	Controller designed for plant G_2
C_3	0.487	1.296	1.463	Controller designed for plant G_3
C_4	0.344	1.317	0.969	Controller designed for plant G_4
C_5	0.227	1.348	0.651	Controller designed for plant G_5
C_6	1.326	1.142	2.733	Spurious controller
C_7	1.102	1.135	1.346	Spurious controller
C_8	1.018	1.132	0.853	Spurious controller
C_9	0.511	1.117	1.067	Spurious controller
C_{10}	0.933	1.132	0.481	Spurious controller

plant output to mimic sensor noise. The frequencies of the excitation signals were selected to bring out the differences in the controllers as the plant parameters deteriorate. Details of other settings used in the simulations are listed below.

- The proposed MMAC with H_∞ cost functional:

$$\theta_j^* = \arg \min_{\theta_j} \max_i \frac{\|(SF_i W^T y)\theta_j - TF_i u\|_{2,\delta}}{\|F_i u\|_{2,\delta}} \quad (13)$$

- A common MMAC with L_2 cost functional on the error signal

$$\theta_j^* = \arg \min_{\theta_j} \|(SW^T y)\theta_j - Tu\|_{2,\delta} \quad (14)$$

- Closed-loop bandwidth: $BW = 0.7 \text{ rad}/\mu\text{sec}$
- Derivate time constant $\tau = 0.01 \mu\text{secs}$
- Forgetting factor (δ) = 5×10^{-4}
- Filter Bank $[F_i]$: 20 filters logarithmically placed between $0.1 \times BW$ and $10 \times BW$
- Hysteresis parameter: $h = 0$
- Frequency of sine wave injected at plant input:
 - $S1$: $0.015 \text{ rad}/\mu\text{sec}$
 - $S2$: $0.15 \text{ rad}/\mu\text{sec}$
 - $S3$: $1.5 \text{ rad}/\mu\text{sec}$

The results of our simulation study are shown in the sequence of figures Fig. 4, 5, 6, for the transition from the plant G_1 to the plants G_2 , G_3 , G_5 , respectively. These plots show the controller index selected by the proposed H_∞ MMAC in a red trace and the index selected by the common L_2 MMAC in a blue trace. Ideally, after an initial transient, we expect both algorithms to converge to the corresponding target controller. It can be clearly seen from these figures that the presence of disturbances cause the L_2 algorithm to fail, while the proposed H_∞ MMAC algorithm converges to correct controller irrespective of the excitation. Some sample output plots are shown in Fig. 7 showing that the proposed MMAC performance is closer to the target. It goes without saying that these are the interesting cases that bring out the difference between the two controllers. Cases with low levels of perturbations or different frequency contents do not produce mis adjustment and are not included here.

5. CONCLUSION

This paper presents an H_∞ -based MMAC algorithm using an approximation of a system norm as a cost functional.

This cost is consistent with the FLS objective used for the initial tuning of all controllers in the controller bank. Then, the controller switching is performed based on minimization of the same cost estimated from input-output data. A buck converter with degradation of its components is used as a motivating example to demonstrate the application proposed algorithm and it is tested under different cases of excitation and disturbances. Our simulation results show that the proposed H_∞ -MMAC algorithm is far less susceptible to the type of excitation and the disturbance, compared to a more common L_2 -MMAC algorithm whose cost objective is based on the error signal (for the same FLS objective).

This result demonstrates the importance of using system-based norms and cost functionals as adaptation metrics,

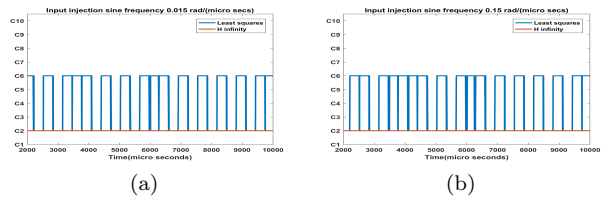


Fig. 4. MMAC results for plant switched from G_1 to G_2 (a) For input injection $S1$ (b) or input injection $S3$; For input injection $S2$ results are similar to of $S1$ and $S3$. For all excitation signals $S1$ - $S3$ the L_2 -based MMAC is switching between the correct controller C_2 and a spurious controller C_6 whereas the H_∞ -MMAC converges to the correct controller C_2

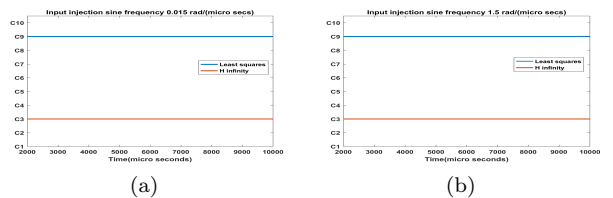


Fig. 5. MMAC results for plant switched from G_1 to G_3 (a) For input injection $S1$, (b) for input injection $S3$; For input injection $S2$ results are similar to of $S1$ and $S3$. For all excitation signals $S1$ - $S3$, the L_2 -MMAC converges to spurious controller C_9 , whereas the H_∞ -MMAC converges to correct controller C_3

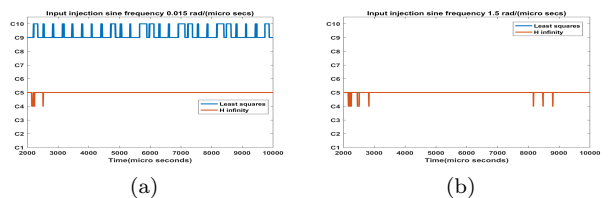


Fig. 6. MMAC results for plant switched from G_1 to G_5 : (a) For input injection $S1$, (b) for input injection $S3$; For input injection $S2$ results are similar to of $S1$. For excitation signals $S1$ and $S2$ the L_2 -MMAC is switching between spurious controller C_9 and C_{10} , while for the excitation signal $S3$ it converges to the correct controller C_5 . The H_∞ -MMAC converges to correct controller C_5 for all excitation signals.

even if they are only approximate. On the other hand, signal-based functionals produce results that are excitation dependent and can be very sensitive to the excitation conditions, especially in perturbed cases. For such cases, looking at ideal-case simulations, or injecting random noise offers little indication of the worst-case behavior. The study of robustness in adaptation should involve signals that are designed specifically to produce misadjustment. Finally, it is also interesting to observe that in these terms of robust performance, multi-model adaptation does not seem to offer an advantage over continuous adaptation. Under perturbed or insufficiently excited conditions, they can both be driven to spurious controllers, if such controllers are contained in the admissible set.

ACKNOWLEDGEMENTS

The authors acknowledge the financial support from the SERDP environmental restoration project 2239.

REFERENCES

Anderson, B., Brinsmead, T., Liberzon, D., and Stephen Morse, A. (2001). Multiple model adaptive control with safe switching. *International journal of adaptive control and signal processing*, 15(5), 445–470.

Anderson, B.D., Brinsmead, T.S., De Bruyne, F., Hespanha, J., Liberzon, D., and Morse, A.S. (2000). Multiple model adaptive control. part 1: Finite controller coverings. *International Journal of Robust and Nonlinear Control*, 10(11-12), 909–929.

Åström, K. and Hägglund, T. (1995). *PID Controllers. Setting the standard for automation*. International Society for Measurement and Control.

Åström, K. and Hägglund, T. (2006). *Advanced PID Control*. ISA-The Instrumentation, Systems, and Automation Society.

Bashivan, P. and Fatehi, A. (2012). Improved switching for multiple model adaptive controller in noisy environment. *Journal of Process Control*, 22(2), 390 – 396.

Böling, J.M., Seborg, D.E., and Hespanha, J.P. (2007). Multi-model adaptive control of a simulated ph neutralization process. *Control Engineering Practice*, 15(6), 663 – 672.

Buchstaller, D. and French, M. (2016a). Robust stability for multiple model adaptive control: Part i - the framework. *IEEE Transactions on Automatic Control*, 61(3), 677–692.

Buchstaller, D. and French, M. (2016b). Robust stability for multiple model adaptive control: Part ii- gain bounds. *IEEE Transactions on Automatic Control*, 61(3), 693–708.

Grassi, E. and Tsakalis, K. (2000). Pid controller tuning by frequency loop-shaping: application to diffusion furnace temperature control. *Control Systems Technology, IEEE Transactions on*, 8(5), 842–847.

Hespanha, J., Liberzon, D., Stephen Morse, A., Anderson, B., Brinsmead, T.S., and De Bruyne, F. (2001). Multiple model adaptive control. part 2: switching. *International journal of robust and nonlinear control*, 11(5), 479–496.

Hespanha, J. and Morse, A. (1996). Supervision of families of nonlinear controllers. In *Decision and Control, 1996., Proceedings of the 35th IEEE Conference on*, volume 4, 3772–3773. IEEE.

Ioannou, P. and Sun, J. (1996). *Robust Adaptive Control*. Number v. 1 in Control theory. PTR Prentice-Hall.

Rivera, D.E., Morari, M., and Skogestad, S. (1986). Internal model control: Pid controller design. *Industrial & engineering chemistry process design and development*, 25(1), 252–265.

Sajjanshetty, K.S. and Safonov, M.G. (2014). Unfalsified adaptive control: Multi-objective cost-detectable cost functions. In *53rd IEEE Conference on Decision and Control*, 1283–1288.

Sastry, S. and Bodson, M. (2011). *Adaptive control: stability, convergence and robustness*. Courier Corporation.

Serrano, V. (2016). *PID Controller Tuning and Adaptation of a Buck Converter*. Arizona State University.

Stefanovic, M. and Safonov, M.G. (2008). Safe adaptive switching control: Stability and convergence. *IEEE Transactions on Automatic Control*, 53(9), 2012–2021.

Tan, C., Yang, H., and Tao, G. (2016). A multiple-model mrac scheme for multivariable systems with matching uncertainties. *Information Sciences*, 360(Supplement C), 217 – 230.

Tsakalis, K. and Dash, S. (2007). Multivariable controller performance monitoring using robust stability conditions. *Journal of Process Control*, 17(9), 702–714.

Tsakalis, K., Dash, S., Green, A., and MacArthur, W. (2002). Loop-shaping controller design from input-output data: application to a paper machine simulator. *Control Systems Technology, IEEE Transactions on*, 10(1), 127–136.

Tsakalis, K.S. (1996). Performance limitations of adaptive parameter estimation and system identification algorithms in the absence of excitation. *Automatica*, 32(4), 549 – 560.

Tsakalis, K.S. and Dash, S. (2013). Approximate h loop shaping in pid parameter adaptation. *International Journal of Adaptive Control and Signal Processing*, 27(1-2), 136–152.

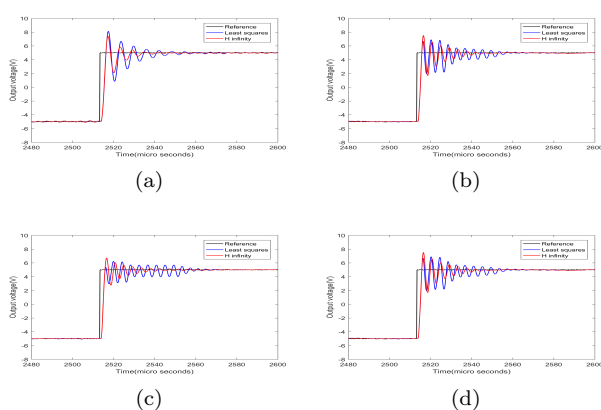


Fig. 7. Output plots of the buck converter: (a) For input injection S_3 for plant switching G_1 to G_3 , (b) for input injection S_2 for plant switching G_1 to G_4 , (c) for input injection S_1 for plant switching G_1 to G_5 , (d) for input injection S_2 for plant switching G_1 to G_5 . In all four cases the proposed H_∞ -MMAC produces tracking performance closer to the target, as compares to the L_2 -based MMAC.